AGU PUBLICATIONS

Geophysical Research Letters

RESEARCH LETTER
10.1002/2015GL063392

Key Points:
- Regional climate model coupled with dynamic glacier parameterization scheme
- Mass balance and ELA for Karakoram-Himalayas glaciers

Supporting Information:
- Text S1 and Table S1
- Figure S1
- Figure S2
- Figure S3
- Figure S4

Correspondence to:
P. Kumar,
pankaj.kumar@hzg.de

Citation:
Kumar, P., S. Kotlarski, C. Moseley, K. Sieck, H. Frey, M. Stoffel, and D. Jacob (2015), Response of Karakoram-Himalayan glaciers to climate variability and climatic change: A regional climate model assessment, *Geophys. Res. Lett.*, *42*, 1818–1825, doi:10.1002/2015GL063392.

Received 6 FEB 2015
Accepted 24 FEB 2015
Accepted article online 26 FEB 2015
Published online 27 MAR 2015

Response of Karakoram-Himalayan glaciers to climate variability and climatic change: A regional climate model assessment

Pankaj Kumar[1], Sven Kotlarski[2], Christopher Moseley[3], Kevin Sieck[3], Holger Frey[4], Markus Stoffel[5], and Daniela Jacob[1]

[1]Climate Service Center 2.0, Helmholtz Zentrum Geesthacht, Hamburg, Germany, [2]Institute for Atmospheric and Climate Science, ETH Zurich, Zurich, Switzerland, [3]Max Planck Institute for Meteorology, Hamburg, Germany, [4]Department of Geography, University of Zurich-Irchel, Zurich, Switzerland, [5]Institute for Environmental Sciences, University of Geneva, Geneva, Switzerland

Abstract The Karakoram and the Himalayan mountain range accommodate a large number of glaciers and are the major source of several perennial rivers downstream. To interactively describe to response of glaciers to climate change, a glacier parameterization scheme has been developed and implemented into the regional climate model REMO. The scheme simulates the mass balance as well as changes of the areal extent of glaciers on a subgrid scale. The parameterization scheme is for the first time applied to the region. A regional glacier inventory is compiled and is used to initialize glacier area and volume. Over the highly complex and data sparse region, the simulated mass balance largely agrees with observations including the positive Karakoram anomaly. The simulated equilibrium line altitude is well captured although a systematic underestimation is apparent. REMO simulates the glacier-climate interaction reasonably well; it has clear potential to be used for future climate assessments.

1. Introduction

Glaciers are key indicators of climate change. Over the Karakoram-Himalayan (K-H) region a large glacier mass exists apart from the Arctic and Antarctic. The region is often referred to as the "water tower of Asia," and is the source of several perennial rivers [*Bolch et al.*, 2012]. These rivers are an important source of water for large populations downstream throughout the year, especially during the dry season [*Siderius et al.*, 2013]. Indian summer monsoon rainfall (ISMR) contributes about 70%–90% to the regional annual rainfall [*Kumar et al.*, 2013]. Over the Karakoram and Western Himalayas, precipitation is mainly received from westerly flows embedded in midlatitude cyclones, regionally called as "western disturbances" [*Mölg et al.*, 2013; *Dimri et al.*, 2013]. Human reach to these mountains is very limited due to its complex terrain and topography, limiting the monitoring of its hydrometeorological and microclimates. The region consists of high topography reaching more than 8000 m. Over high mountains the network of meteorological data recording stations is very sparse; most of them are placed in valleys or at lower altitudes. Hence, observed precipitation estimates over this region are likely to be highly underestimated as a consequence of the general increase of precipitation with altitude in combination with the sampling of low-elevation stations only [*Winiger et al.*, 2005; *Immerzeel et al.*, 2012; *Palazzi et al.*, 2013; *Maussion et al.*, 2013]. Figure 1 shows the observational precipitation (Asian Precipitation - Highly-Resolved Observational Data Integration Towards Evaluation (APHRODITE)) station network over the region of study. Over the Karakoram (>5000 m) there is no single station, similarly in large parts of the Western Himalayas and Tibet. Therefore, it is a great challenge to prepare gridded data from the available station network for this region. Satellite-derived data may provide a better estimate; however, they do have difficulties in estimating the snow contribution [*Rasmussen et al.*, 2012], which constitutes an important component of total precipitation over this region throughout almost the entire year. For this region, an alternative to observational data may be reanalysis products. These are produced using state-of-art global circulation models and data assimilation techniques, trying to keep the simulated data close to the available observations. They take care of both components of precipitation (i.e., rainfall and snowfall) at each grid box and are physically consistent.

Modeling the response of glaciers in the K-H region to climate variability and climate change is even a greater challenge. The direct applicability of global and regional climate models (GCMs and RCMs) for this purpose is limited as most GCMs/RCMs apply static glacier masks and do not treat glaciers as an interactive component of the climate system. However, some recent Earth system models (updated GCMs) do have an

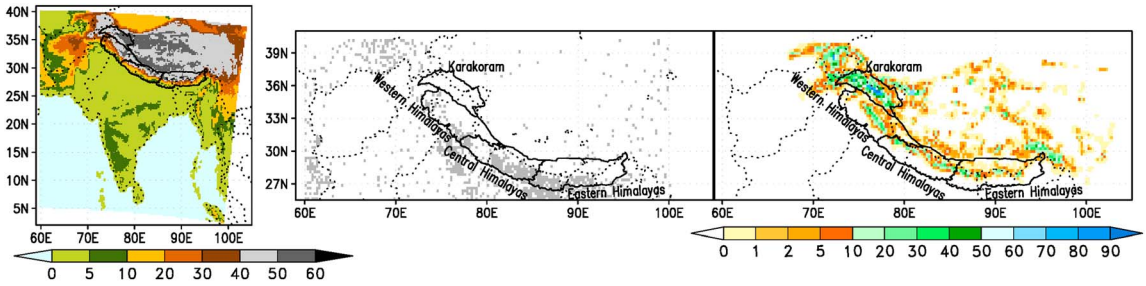

Figure 1. (left) Model domain and subgrid orography (m × 100). (middle) APHRODITE station locations (each REMO grid box that includes at least one measurement station is colored in gray). (right) Glacier inventory, showing fraction of glacier cover in each $REMO_{glacier}$ grid box on 1 January 1989.

ice sheet model coupled but they are available at horizontal grid resolutions of ~200 × 200 km only. In offline approaches, GCM and RCM output can be used to estimate past, present, and future changes in the meteorological forcing and their respective influence on glacier mass balance [e.g., *Mölg and Kaser*, 2011; *Wiltshire*, 2014; *Kapnick et al*., 2014]. Alternatively, RCMs embedded with an online and interactive glacier parameterization scheme may provide physically consistent mass balance information over such a complex terrain and highly data sparse region. However, at present only few such model systems are available [*Kotlarski et al*., 2010; *Collier et al*., 2013]. The coupled model scheme $REMO_{glacier}$ [*Kotlarski et al*., 2010] has been developed for the European Alps, but has not been used outside this region so far. The objective of the present paper is to apply and validate $REMO_{glacier}$ for the first time over the K-H region and to assess the suitability of the coupled climate-glacier model system with the aim to apply it for future scenarios of climate and glacier changes.

2. Model Method and Data

2.1. REMO

The Regional Climate Model (REMO) is a limited-area three-dimensional hydrostatic model of the atmosphere [*Jacob*, 2001, 2009]. REMO combines the physical parameterization scheme of the Max Planck Institute for Meteorology GCM ECHAM versions 4 and 5 [*Roeckner et al*., 1996, 2003] and the dynamical core of the former forecast model of the German Weather Service (Europamodell [*Majewski*, 1991]). In the standard RCM setup individual grid boxes consist of land, water, and sea ice fractions. This technique allows to account for the subgrid-scale variability due to different land surface types (http://www.remo-rcm.de/). In the standard REMO setup, glaciers and ice sheets are represented by a static glacier mask which is constant in time, as it is done by most state-of-the-art global and regional models.

2.2. Glacier Scheme

Kotlarski et al. [2010] developed and applied an online glacier parameterization scheme that is fully coupled to the atmospheric and land surface component of REMO. The coupled model system is referred to as $REMO_{glacier}$. The scheme represents surface glacier cover on a subgrid scale and calculates the energy and mass balance of the glacierized part of a grid box. This part is allowed to grow and shrink dynamically depending on the simulated mass balance but is restricted to the total land surface area of the respective grid box. All glaciers located in a given RCM grid box are combined to a single, two-layer ice cuboid with area "A" and height "h" covering a certain fraction of the total grid box area. Mass balance occurs uniformly over the glacier cuboid surface. This simplification is motivated by the fact that nearby glaciers often show a similar response to a given climate forcing [*Cogley and Adams*, 1998]. However, it also means a neglect of any subgrid variability of glacier mass balance which can, for instance, be introduced by elevation and slope effects. The glacier cuboid surface can additionally be covered by a snow layer. It is assumed to be located at the mean grid box altitude which is constant throughout the simulation. Hence, the effect of a possible surface elevation-mass balance feedback is not taken into account. Simulated mass balance is expressed in terms of the mean specific mass balance. Accumulation terms are snowfall and rime formation, whereas ablation occurs by snow and ice melt calculated by an energy balance approach (see below). Snow metamorphism is not explicitly considered; instead, the transformation from snow to ice is parameterized in terms of the snow age. The surface energy balance for the glacierized grid box fraction at each time step is computed as

$$dQice/snow = K + L + H + LE + G + M \quad (1)$$

where K is net shortwave radiation, L is net longwave radiation, H is turbulent sensible heat flux, LE is turbulent latent heat flux, G is ground heat flux, M is amount of energy consumed during melt of snow and ice, and dQice/snow is the energy change of heat content in the upper snow or ice layer. Snow and ice melt occurs once the temperature of the respective layer exceeds the melting point of 0°C. Glacier thickness (or volume, respectively) and area are related to each other by a power law. Large-scale ice flow across grid box boundaries is neglected. Also, the effect of debris cover on the glacier surface albedo is not accounted for. For further details on the glacier parameterization scheme refer to *Kotlarski* [2007] and *Kotlarski et al.* [2010].

2.3. Glacier Inventory

A glacier inventory was prepared for the glacierized part of the RCM domain (Figure 1). It comprises all mountain ranges in the region. Glacier data were collected from the Global Land Ice Measurements from Space database [*Raup et al.*, 2007; www.glims.org], glacier data published by the *International Centre for Integrated Mountain Development* [2007], and Environmental Systems Research Institute's Digital Chart of the World [*Danko*, 1992]. Data quality, acquisition dates, and glacier parameters provided are heterogeneous; in case of overlapping coverage, the database with the highest quality was selected. Glacier areas were derived from glacier polygons, and topographic parameters, such as mean slope, were derived from the void-filled version of the Shuttle Radar Topography Mission digital elevation model [*Reuter et al.*, 2007] and the slope and aspect grids derived thereof. Despite differing acquisition dates, the inventory is assumed to represent glacier conditions from around 1990. Our inventory covers a glacierized fraction of 98,504 km^2, which corresponds to the 100,000 km^2 given in *Yao et al.* [2012]. The present study focuses on the K-H region. Based on *Bolch et al.* [2012], the K-H region is further subdivided into four parts, namely, Karakoram (K), Western Himalaya (WH), Eastern Himalaya (EH), and Central Himalaya (CH) (Figure 1).

2.4. Experimental Design

$REMO_{glacier}$ was integrated over South Asia (Figure 1) for the period 1989–2008 at a horizontal resolution of 0.22° × 0.22° (~25 km) with 27 vertical levels and driven by the ERA-Interim (ERAI) reanalysis [*Dee et al.*, 2011] at the lateral boundaries. Glacier inventory data were used to initialize the glacierized grid box fraction at the very first time step. The analysis focuses on simulated annual and seasonal (winter (December-January-February), spring (March-April-May), summer (June-July-August), and autumn (September-October-November)) mean statistics of atmospheric and glaciological quantities. ERAI and $REMO_{glacier}$ simulated precipitation are analyzed with respect to total precipitation and rainfall part only (no snow).

2.5. Data Used

Model results are compared against several gridded station observation data of precipitation and temperature, namely CRU_v3.1 [*Harris et al.*, 2014], University of Delaware (UDW) (http://www.esrl.noaa.gov/psd/data/gridded/data.UDel_AirT_Precip.html), APHRODITE [*Yatagai et al.*, 2012; *Yasutomi et al.*, 2011], and Global Precipitation Climatology Centre (GPCC) (http://gpcc.dwd.de). Hereafter all gridded station data will be referred to as "observations." Due to the lack of reliable observational network, we also include reanalysis data into analysis, namely, ERAI and Modern Era Retrospective-Analysis for Research and Applications (MERRA) [*Rienecker et al.*, 2011]. Model results are validated against MERRA. Table S1 in the supporting information provides details on observational and reanalysis data and their precipitation and temperature statistics with $REMO_{glacier}$.

3. Result and Discussion

3.1. Precipitation and Temperature

The simulated annual cycles of precipitation and temperature over the K-H region are shown in Figure 2 along with those of the reference data. The annual cycle is well represented by $REMO_{glacier}$, i.e., lowest precipitation extending from December to spring, followed by a sharp increase in summer due to the influence of ISMR. With respect to the observations, the model is showing an overestimation of precipitation throughout the year, but it agrees reasonably well with MERRA. The region receives the maximum precipitation in summer, suggesting that it is dominated by monsoon climate. However, over the subdomain Karakoram, the annual cycle of precipitation is dominated by winter precipitation, with moist conditions extending from September to May, followed by a sharp decrease during summer as the influence of monsoon currents is very small. Most of the precipitation received (approximately 90%) over the region is snowfall, especially above

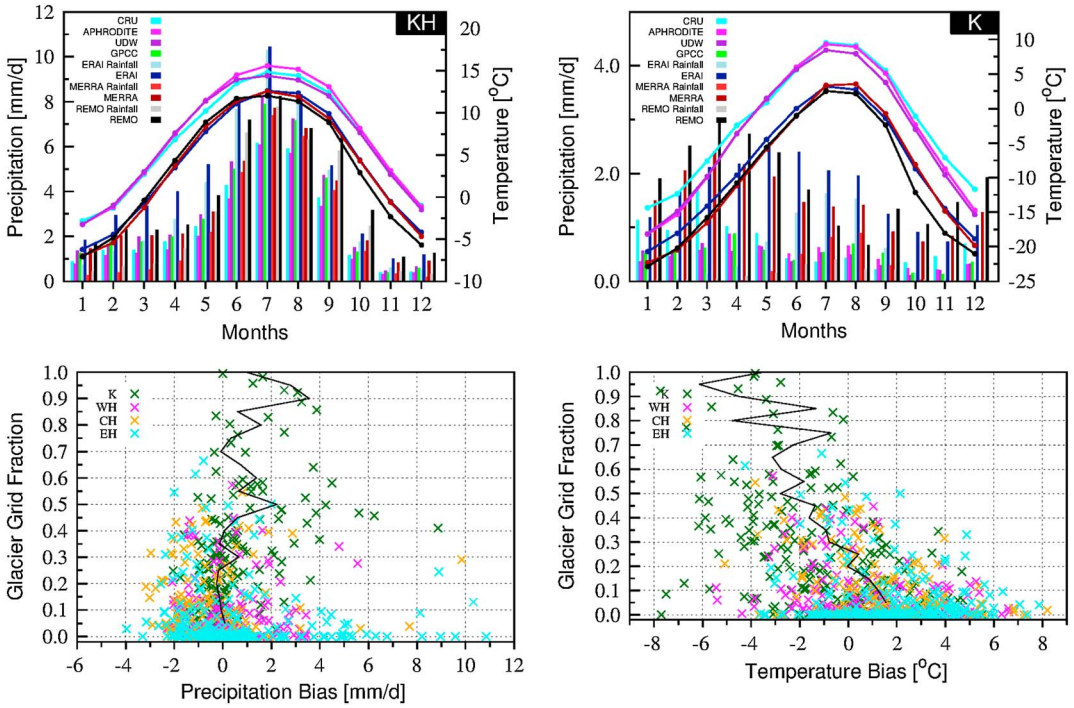

Figure 2. (top row) Mean annual cycle (1989–2007) of precipitation (bars) and temperature (lines) over the entire K-H region (left) and the Karakoram (right). MERRA/ERAI/REMO$_{glacier}$ simulated precipitation is analyzed for both total precipitation (MERRA/ERAI/REMO) and rainfall (MERRA Rainfall/ERAI Rainfall/REMO Rainfall) (no snow). (bottom row) The annual mean precipitation bias (left) and temperature bias (right) with respect to MERRA against glacierized grid box fraction for the four analysis domains. The solid line shows the annual mean bias at every 5% interval of mean glacierized grid box fraction.

5000 m [*Winiger et al.*, 2005]. Over the Karakoram REMO$_{glacier}$ produces 20% more annual mean precipitation than MERRA and approximately 150% to 300% more than the observations (Table S1). The model simulates two peaks in the precipitation annual cycle over WH and CH as is shown by the observations, and the annual cycle of temperature is reasonably well reproduced over all regions (Figure S1). Throughout the entire year the mode produces a negative temperature bias over all subregions with respect to observations. When compared to MERRA, the annual cycle is well captured, though model is showing a negative bias of nearly ~1°C in winter, probably leading to an overestimation of the fraction of solid precipitation. Over the K-H region, significance test of yearly mean temperature and precipitation as given by REMO$_{glacier}$, MERRA, and observations show a large agreement between data sets on a significant (95% level) positive temperature trend for the period 1989–2007, although the driving ERAI reanalysis shows a negative trend. By contrast, the period is too short to make significant statements about precipitation trends. Precipitation spatial heterogeneity is well simulated by the model (Figure S2), e.g., orographic precipitation or the precipitation band over the windward side of the Himalayas. Over the Karakoram, precipitation is mainly received from westerly flows embedded in midlatitude cyclones. When the moisture-laden wind strikes the high mountains, it produces precipitation at their windward sides. In this region, REMO$_{glacier}$ simulates more winter precipitation than shown by observations (Figures 1, left, and S2, top left). Topographic precipitation is well represented by the model, which feeds the large glaciers in winter and enables them not only to sustain its mass but can lead to a positive mass balance, the so-called "*Karakoram anomaly*" [*Hewitt*, 2005]. MERRA shows overall precipitation magnitudes and patterns comparable to those of REMO$_{glacier}$ but cannot represent grid boxes with very high orographic precipitation due to lower resolution. ERAI captures the general precipitation magnitude, but, same as for MERRA, its horizontal resolution is coarser than that of REMO$_{glacier}$ and the spatial variability is therefore less pronounced. Observations are unable to capture the local topographic features and for instance show hardly any precipitation over the Karakoram, which is probably reflective of the limited number of measuring stations (Figure 1) and the systematic gauge undercatch. Therefore, we thus conclude that REMO$_{glacier}$ simulated winter precipitation over the Karakoram more realistically than precipitation patterns suggested by observations and reanalysis data.

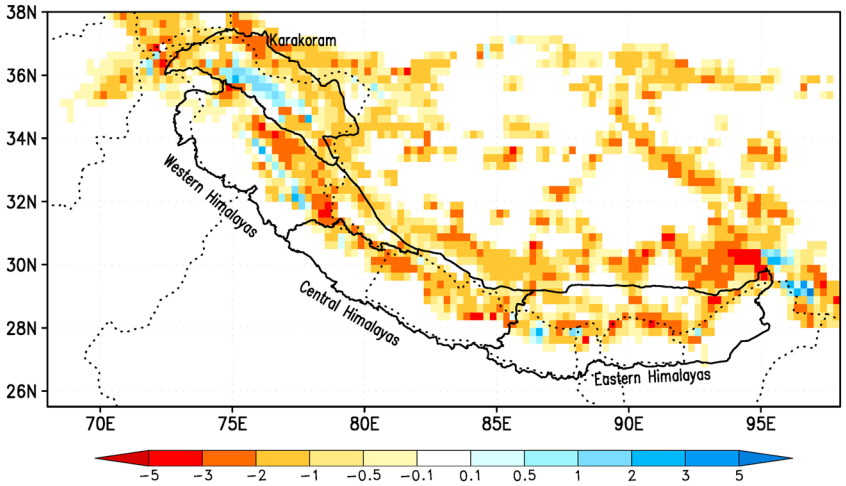

Figure 3. Simulated mean annual mass balance (meters water equivalent (mwe)) for the period 1989–2008.

3.2. Precipitation and Temperature Bias Over Four Regions

Figure 2 shows the mean annual bias of simulated precipitation over glacierized grid boxes of the four regions with respect to MERRA. Generally, a mean bias of 0.5 mm/d over glacierized grid box fractions $<$40% is seen over all regions. $REMO_{glacier}$ for the K-H region as a whole overestimates precipitation by 23% to 74% with respect to the observations, whereas with respect to MERRA by 22% (Table S1). These numbers highlight the large uncertainty in determining "true" precipitation sums in the region. In the Karakoram, glacierized grid boxes show a consistent positive precipitation bias especially for highly glacierized grid boxes that receive large amounts of precipitation at high mountain ranges. The model bias is smaller where the number of observational stations is larger (Figure 1), e.g., over EH and CH compared to Karakoram (Table S1). A seasonal analysis over grid boxes shows an underestimation of precipitation over WH and CH in summer (Figure S3), whereas during the rest of the year precipitation is largely overestimated.

The temperature bias over glacierized grid boxes is shown in Figure 2. For fair comparison, MERRA data are height corrected to the $REMO_{glacier}$ topography using a standard lapse rate of 6.5 K/km. $REMO_{glacier}$ simulates generally a cooler climate over highly glacierized grid boxes. For grid boxes with small glacier cover ($<$50%) the mean bias is in the range of $-$2°C to 2°C, whereas for some highly glacierized grid boxes it reaches up to $-$7°C. The seasonal temperature bias (Figure S4) is very similar to the annual bias, although the bias magnitude varies seasonwise. Biases in some grid boxes reach $-$10°C in autumn. This negative bias increases with increasing glacierized grid fraction.

In summary, over the data sparse and topographically complex K-H region, the RCM seems to be able to capture the areal extent and magnitude of precipitation realistically. However, observed precipitation sums are mostly overestimated, especially in the seasons where the largest fraction of total precipitation is expected to be snow. This is likely to be even further increased by the model's cold bias in winter and probably feeds back to the cold temperature bias in the RCM. However, the role of MERRA's coarser horizontal resolution should be kept in mind when interpreting $REMO_{glacier}$'s apparent precipitation bias. Therefore, the apparent positive model overestimation might actually not be a real overestimation. We even argue that, as a result of the complexity of the system high-resolution models like $REMO_{glacier}$ may provide more "realistic" local climate estimates for such heterogeneous regions [*Ménégoz et al.*, 2013].

3.3. Mass Balance Studies

Anthropogenic climate change is likely to accelerate the receding of Himalayan glaciers as projected temperature changes over this region are larger than in the surrounding plains [*Kumar et al.*, 2013]. Mass balance is a key indicator of glacier change and retreat. The $REMO_{glacier}$ simulated mass balance is assumed to represent the mean specific mass balance averaged over all individual glaciers in a given model grid box. Over this highly data sparse region, no observation base exists to compare the simulated results as a whole. Therefore, in terms of glacier mass balance we cannot directly compare our results with any observation.

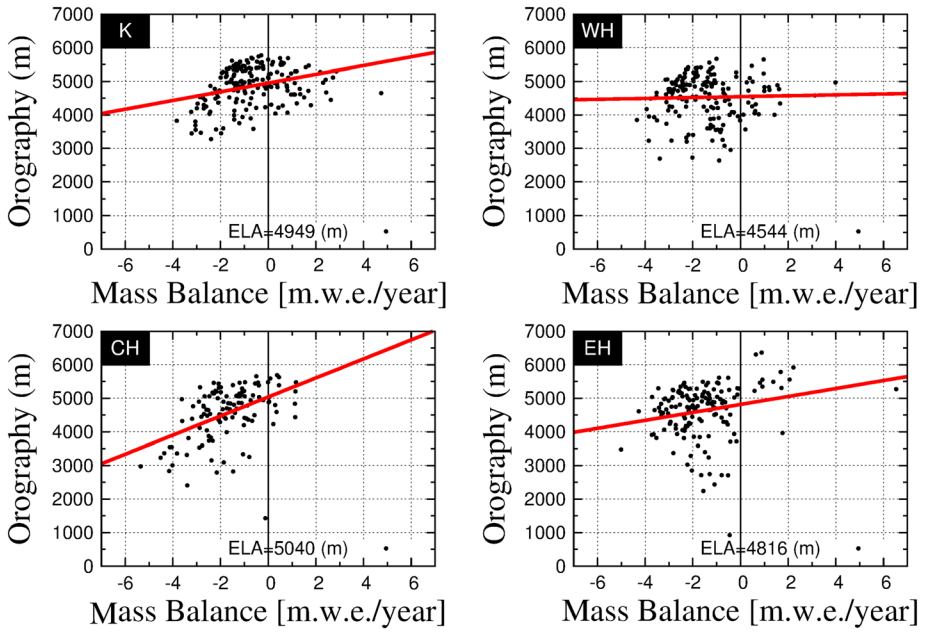

Figure 4. Simulated mean annual mass balance (mwe/yr) against grid box orography (m), for the period 1989–2008. The point where mass balance is zero on the regression line is considered as an estimate of the regional ELA of the respective domain.

However, some mass balance data are available for individual glaciers or smaller subregions. We here use data from published mass balance studies over the Himalayas to validate the $REMO_{glacier}$ results. Figure 3 shows the spatial map of simulated mean annual mass balance (1998–2008) of ice and snow over the glacierized grid fraction over the K-H region. $REMO_{glacier}$ simulates a negative mass balance over most parts of the region, especially over CH, EH, and Tibet. A positive mass balance anomaly (windward side) is simulated over the Karakoram and Kunlun mountain ranges (east of Karakoram), whereas the overall mass balance for the Karakoram region is negative. Both ranges are located above approximately 5000 m and are mainly fed by winter precipitation. This positive mass balance anomaly simulated by the model seems to agree with other reported studies based on in situ and satellite-derived information [*Hewitt*, 2005; *Bolch et al*., 2012; *Gardelle et al*., 2012; *Neckel et al*., 2014]. This is an import result as the model is not only able to simulate the reported mean negative mass balance over K-H but also the reported positive mass balance anomaly in the Karakoram. There are some grid boxes (10–15 in number) where a positive mass balance anomaly over the K-H region is simulated, which have not been reported by any study so far. However, *Jacob et al*. [2012] found almost balanced mass changes based on Gravity Recovery and Climate Experiment data. It is a known artifact of RCMs without filtered topography, including REMO that they have the tendency to overestimate orographic precipitation where large differences in surface elevation between neighboring grid boxes occur. In the case of advection and/or (numerical) diffusion of moisture from the lower to the higher grid box usually warmer and moister air is forced to lift which often leads to excessive precipitation over the higher elevated box. In some of the cases with positive mass balance discussed above, this effect could play a role and lead to a strong positive bias of snow accumulation. Thus, heavily glaciated grid boxes experience strong snow accumulation, which subsequently turns into ice, leading to an increase in total ice depth, area, and volume. In $REMO_{glacier}$, the interaction between two grid boxes is not implemented; hence, the ice flow to lower ablation areas is neglected. Especially for high-elevated grid boxes this can lead to a permanent positive mass balance. One example for this effect is seen in the WH and EH (Figure 3).

3.4. Equilibrium Line Altitude

The equilibrium line is a theoretical line which marks the region where glacier mass balance is zero, that is, the region which divides the net snow and ice gain (accumulation) zone from the loss (ablation) zone in a particular year (or period). Its altitude is referred to as equilibrium line altitude (ELA). Over K-H the observation-based ELA estimates range from 4400 m to 5700 m [*Bolch et al*., 2012; *Yao et al*., 2012]. As the glacier scheme currently

includes no subgrid topography, it is not possible to derive the ELA for individual grid boxes. However, the regional-scale ELA can be obtained by plotting the mean annual mass balance against grid box elevation for each glacierized grid box in the domain. On a simple scatterplot, the ELA is defined as the elevation where the mass balance is zero. Simulated ELAs referring to mean glacier mass balances for the period 1989–2008 are presented in Figure 4. The model is able to approximately represent the ELA for the selected subregions when compared to observed values. The expected positive relation between altitude and mass balance is reproduced by the model. The $REMO_{glacier}$ estimated ELA for Karakoram is 4949 m, 4544 m for WH, 5040 m for CH, and 4816 m for EH. All these values are close to those reported (*Yao et al*. [2012] (4800 m to 5200 m) and *Bolch et al*. [2012] (5150 m to 5600 m)), and a slight systematic underestimation is apparent. This would mean that the simulated regional mean mass balance is larger than the true mass balance.

4. Conclusions

For the first time we present a complete simulation of glacier-climate interaction over South Asia. The regional climate model ($REMO_{glacier}$), which includes a dynamical glacier parameterization scheme ("dynamic" in terms of an interactive temporal evolution of glacier characteristics), is initialized by a glacier inventory, which is interpolated to the RCM grid and represents the glacierized fraction within every model grid box. The Karakoram-Himalayas are a highly data sparse region which limits the proper cross validation of RCM results. Keeping these restrictions in mind, the RCM shows very good skill in simulating the areal extent of precipitation and physically explainable patterns (e.g., Karakoram anomaly). However, $REMO_{glacier}$ results are also subject to a number of apparent limitations related to (i) an overestimation of orographic precipitation in some grid boxes due to sharp orographical gradients from grid box to grid box (500 m to 1400 m in some cases), (ii) a neglection of subgrid variability of atmospheric forcing parameters for the embedded glacier scheme, and (iii) uncertainties of the observational glacier inventory used to initialize glaciers in the RCM. The spatial patterns of simulated glacier mass balance show an overall negative mass balance but also reveal regions with positive mass balance anomalies especially over the Karakoram. For parts of the domain this is in agreement with previous works. In other cases, the positive mass balance bias can likely be related to biases in the simulated atmospheric forcing, especially to an overestimation of (solid) precipitation sums. The positive relation between altitude and mass balance is qualitatively reproduced by the model. $REMO_{glacier}$ is able to approximately represent the ELA although the simulated ELAs seem to have a slight systematic negative bias. This is consistent with the overestimation of the mean regional mass balance. In general, this first evaluation of the coupled $REMO_{glacier}$ modeling system over the Karakoram-Himalayan region provides confidence in the model setup and in its general applicability for future climate and glacier change studies over the K-H region.

Acknowledgments

This study was partially supported by the funding from the Federal Ministry of Education and Research, Germany, for GLACINDIA project (contract 033L164), the EU-FP7 HighNoon project (contract 227087), and the SDC GPCC project IHCAP. We acknowledge DKRZ Germany for providing CPU time for $REMO_{glacier}$ simulations. All the observational data used in the study are freely available. Model data and a glacier inventory used in the analysis are available freely and, if needed, can be provided by the first author. We are thankful to the anonymous three referees for their constructive and useful comments.

The Editor thanks three anonymous reviewers for their assistance in evaluating this paper.

References

Bolch, T., et al. (2012), The state and fate of Himalayan glaciers, *Science*, *336*(6079), 310–314, doi:10.1126/science.1215828.

Cogley, J. G., and W. P. Adams (1998), Mass balance of glaciers other than the ice sheets, *J. Glaciol.*, *44*(147), 315–325.

Collier, E., T. Mölg, F. Maussion, D. Scherer, C. Mayer, and A. G. B. Bush (2013), High-resolution interactive modelling of the mountain glacier-atmosphere interface: An application over the Karakoram, *Cryosphere*, *7*(3), 779–795, doi:10.5194/tc-7-779-2013.

Danko, D. M. (1992), The digital chart of the world project, *Photogramm. Eng. Remote Sens.*, *58*(8), 1125–1128.

Dee, D. P., et al. (2011), The ERA-interim reanalysis: Configuration and performance of the data assimilation system, *Q. J. R. Meteorol. Soc.*, *37*, 553–597, doi:10.1002/qj.828.

Dimri, A. P., T. Yasunari, A. Wiltshire, P. Kumar, C. Mathison, J. Ridley, and D. Jacob (2013), Application of regional climate models to the Indian winter monsoon over the western Himalayas, *Sci. Total Environ.*, *468–469*, 36–47, doi:10.1002/joc.3584.

Gardelle, J., E. Berthier, and Y. Arnaud (2012), Slight mass gain of Karakoram glaciers in the early twenty-first century, *Nat. Geosci.*, *5*, 322–325, doi:10.1038/ngeo1450.

Harris, I., P. D. Jones, T. J. Osborn, and D. H. Lister (2014), Updated high-resolution grids of monthly climatic observations—The CRU TS3.10 dataset, *Int. J. Climatol.*, *34*, 623–642, doi:10.1002/joc.3711.

Hewitt, K. (2005), The Karakoram anomaly? Glacier expansion and the "elevation effect," Karakoram Himalaya, *Mt. Res. Dev.*, *25*(4), 332–340, doi:10.1659/0276-4741(2005)025%5B0332:TKAGEA%5D2.0.CO;2.

Immerzeel, W. W., F. Pellicciotti, and A. B. Shrestha (2012), Glaciers as a proxy to quantify the spatial distribution of precipitation in the Hunza basin, *Mt. Res. Dev.*, *32*(1), 30–38, doi:10.1659/MRD-JOURNAL-D-11-00097.1.

International Centre for Integrated Mountain Development (2007), Inventory of glaciers, glacial lakes and identification of potential glacial lake outburst floods (GLOFs) affected by global warming in the mountains of Himalayan region (DVD-ROM) Kathmandu, Nepal.

Jacob, D. (2001), A note to the simulation of the annual and interannual variability of the water budget over the Baltic Sea drainage basin, *Meteorol. Atmos. Phys.*, *77*, 61–73, doi:10.1007/s007030170017.

Jacob, D. (2009), *Regional Climate Models: Linking Global Climate Change to Local Impacts; The Springer Encyclopedia of Complexity and Systems Science*, pp. 7591–7602, Springer, Berlin, New York, doi:10.1007/978-0-387-30440-3_449.

Jacob, T., J. Wahr, W. T. Pfeffer, and S. Swenson (2012), Recent contributions of glaciers and ice caps to sea level rise, *Nature*, *482*, 514–518, doi:10.1038/nature10847.

Kapnick, S. B., T. L. Delworth, M. Ashfaq, S. Malyshev, and P. C. D. Milly (2014), Snowfall less sensitive to warming in Karakoram than in Himalayas due to a unique seasonal cycle, *Nat. Geosci.*, *7*, 834–840, doi:10.1038/ngeo2269.

Kotlarski, S. (2007), A subgrid glacier parameterisation for use in regional climate modelling, PhD thesis, Reports on Earth System Science, 42, Univ. of Hamburg, Max Planck Inst. for Meteorol., Hamburg, Germany. [Available at http://www.mpimet.mpg.de/fileadmin/publikationen/Reports/WEB_BzE_42.pdf.]

Kotlarski, S., D. Jacob, R. Podzun, and F. Paul (2010), Representing glaciers in a regional climate model, *Clim. Dyn.*, *34*, 27–46, doi:10.1007/s00382-009-0685-6.

Kumar, P., et al. (2013), Downscaled climate change projections with uncertainty assessment over India using a high resolution multi-model approach, *Sci. Total Environ.*, *468–469*, 18–30, doi:10.1016/j.scitotenv.2013.01.051.

Majewski, D. (1991), The Europa-Modell of the Deutscher Wetterdienst, in *ECMWF Seminar on Numerical Methods in Atmospheric Models*, vol. 2, pp. 147–191, Reading, U. K. [Available at http://www.pa.op.dlr.de/cleocd/dwdmod/s.htm.]

Maussion, F., D. Scherer, T. Mölg, E. Collier, J. Curio, and R. Finkelnburg (2013), Precipitation seasonality and variability over the Tibetan Plateau as resolved by the High Asia Reanalysis, *J. Clim.*, *27*, 1910–1927. [Available at http://journals.ametsoc.org/doi/abs/10.1175/JCLI-D-13-00282.1.]

Ménégoz, M., H. Gallée, and H. W. Jacobi (2013), Precipitation and snow cover in the Himalaya: From reanalysis to regional climate simulations, *Hydrol. Earth Syst. Sci.*, *17*, 3921–3936, doi:10.5194/hess-17-3921-2013.

Mölg, T., and G. Kaser (2011), A new approach to resolving climate-cryosphere relations: Downscaling climate dynamics to glacier-scale mass and energy balance without statistical scale linking, *J. Geophys. Res.*, *116*, D16101, doi:10.1029/2011JD015669.

Mölg, T., F. Maussion, and D. Scherer (2013), Mid-latitude westerlies as a driver of glacier variability in monsoonal High Asia, *Nat. Clim. Change*, *4*, 68–73, doi:10.1038/nclimate2055.

Neckel, N., J. Kropáček, T. Bolch, and V. Hochschild (2014), Glacier mass changes on the Tibetan Plateau 2003–2009 derived from ICESat laser altimetry measurements, *Environ. Res. Lett.*, *9*, doi:10.1088/1748-9326/9/1/014009.

Palazzi, E., J. von Hardenberg, and A. Provenzale (2013), Precipitation in the Hindu-Kush Karakoram Himalaya: Observations and future scenarios, *J. Geophys. Res. Atmos.*, *118*, 85–100, doi:10.1029/2012JD018697.

Rasmussen, R., et al. (2012), How well are we measuring snow?, *Bull. Am. Meteorol. Soc.*, *93*, 811–829, doi:10.1175/BAMS-D-11-00052.1.

Raup, B., A. Racoviteanu, S. Khalsa, C. Helm, R. Armstrong, and Y. Arnaud (2007), The GLIMS geospatial glacier database: A new tool for studying glacier change, *Global Planet. Change*, *56*(1–2), 101–110.

Reuter, H. I., A. Nelson, and A. Jarvis (2007), An evaluation of void filling interpolation methods for SRTM data, *Int. J. Geogr. Inf. Sci.*, *21*(9), 983–1008, doi:10.1080/13658810601169899.

Rienecker, M. M., et al. (2011), MERRA: NASA's Modern-Era Retrospective Analysis for Research and Applications, *J. Clim.*, *24*, 3624–3648, doi:10.1175/JCLI-D-11-00015.1.

Roeckner, E., K. Arpe, L. Bengtsson, M. Christoph, M. Claussen, L. Dümenil, M. Esch, M. Giorgetta, U. Schlese, and U. Schulzweida (1996), The atmospheric general circulation model ECHAM-4: Model description and simulation of present-day climate, *Rep. 218*, Max Planck Inst. for Meteorol. [Available at https://www.mpimet.mpg.de/fileadmin/publikationen/Reports/MPI-Report_218.pdf.]

Roeckner, E., et al. (2003), The atmospheric general circulation model ECHAM 5. Part I: Model description, *Rep. 349*, MPI for Meteorol., Hamburg, Germany.

Siderius, C., H. Biemans, A. Wiltshire, S. Rao, W. Franssen, P. Kumar, A. K. Gosain, M. T. van Vliet, and D. N. Collins (2013), Snowmelt contributions to discharge of the Ganges, *Sci. Total Environ.*, *468–469*, 93–101, doi:10.1016/j.scitotenv.2013.05.084.

Wiltshire, A. J. (2014), Climate change implications for the glaciers of the Hindu Kush, Karakoram and Himalayan region, *Cryosphere*, *8*, 941–958, doi:10.5194/tc-8-941-2014.

Winiger, W., M. Gumpert, and H. Yamout (2005), Hydrological processes, *Hydrol. Process.*, *19*, 2329–2338, doi:10.1002/hyp.5887.

Yao, T., et al. (2012), Different glacier status with atmospheric circulations in Tibetan Plateau and surroundings, *Nat. Clim. Change*, *2*, 663–667, doi:10.1038/nclimate1580.

Yasutomi, N., A. Hamada, and A. Yatagai (2011), Development of a long-term daily gridded temperature dataset and its application to rain/snow discrimination of daily precipitation, *Global Environ. Res.*, *15*(2), 165–172. [Available at http://www.chikyu.ac.jp/precip/data/Yasutomi2011GER.pdf.]

Yatagai, A., K. Kamiguchi, O. Arakawa, A. Hamada, N. Yasutomi, and A. Kitoh (2012), APHRODITE: Constructing a long-term daily gridded precipitation dataset for Asia based on a dense network of rain gauges, *Bull. Am. Meteorol. Soc.*, *93*, 1401–1415, doi:10.1175/BAMS-D-11-00122.1.